

https://dspace.org/

Pongola Supergroup dolostones from the Buffalo River inlier South Africa facies composition and implications for Mesoarchaean carbonate deposition

M Siahi; A Hofmann; J Dixon; Allan Wilson; E et al

ELSEVIER SCIENCE BV
https://hdl.handle.net/10539/43082
WOS

Downloaded from a DSpace repository. https://dspace.org/

Precambrian Research 411 (2024) 107493

Contents lists available at ScienceDirect

Precambrian Research

journal homepage: www.elsevier.com/locate/precamres

Pongola Supergroup dolostones from the Buffalo River inlier, South Africa: facies, composition and implications for Mesoarchaean carbonate deposition

M. Siahi [a,b,c], A. Hofmann [c,*], J. Dixon [d], A. Wilson [e], C. Mayr [b,f], L. Kapesi [g]

[a] Energetic Materials, Rock Characterization, and Geomechanics, Missouri University of Science and Technology, United States
[b] Department of Earth and Environmental Sciences, Ludwig-Maximilian-University, Munich, Germany
[c] Department of Geology, University of Johannesburg, Johannesburg, South Africa
[d] School of Geological Sciences, University of KwaZulu-Natal, Durban, South Africa
[e] School of Geosciences, University of the Witwatersrand, Johannesburg, South Africa
[f] Department of Geography and Earth Sciences, Friedrich-Alexander-University of Erlangen-Nürnberg, Erlangen, Germany
[g] ASSORE Raman Laboratory, Palaeoproterozoic Mineralization Research Group, Department of Geology, University of Johannesburg, Johannesburg, South Africa

ARTICLE INFO

Keywords:
Kaapvaal Craton
Pongola Supergroup
Buffalo River inlier
Mesoarchaean
Stromatolitic carbonate rocks

ABSTRACT

The Mesoarchaean Pongola Supergroup of South Africa hosts the oldest succession of stromatolitic carbonates deposited in an intracontinental setting. In this study, carbonates within two (tectono-)stratigraphic units in the Buffalo River inlier were investigated. Stratiform stromatolite and ripple-laminated dolostone facies are the most common and are interpreted to have formed in a tide-dominated shallow-marine environment. Dolostones typically contain a large amount of siliciclastic detritus, and small domal stromatolites are commonly found scattered in subtidal sandstone facies. The carbonates experienced deformation and greenschist facies metamorphic conditions at peak temperatures of ~450 ± 50 °C. Analyses for major, trace and rare earth elements (REE) along with carbon, oxygen and strontium isotopes have been undertaken on the best-preserved samples. Their REE + Y distribution patterns reflect their marine origin, with positive La_{SN}, Gd_{SN} and Y_{SN} anomalies, super-chondritic Y/Ho ratios, and depleted light REE relative to heavy REE. The $\delta^{13}C_{VPDB}$ and $\delta^{18}O_{VPDB}$ values least affected by diagenetic and metamorphic overprints are 2.2 ‰ and −16.1 ‰, respectively. The least radiogenic $^{87}Sr/^{86}Sr$ ratio is 0.704 and reflects isotopic exchange with a siliciclastic component. Despite their alteration, the carbonates of the Buffalo River inlier provide additional constraints on microbial carbonate deposition on the Earth oldest preserved craton. They can be traced laterally for several tens of kilometres and point to environmental conditions suitable for the deposition and preservation of marine carbonate rocks 3.0 Ga ago.

1. Introduction

The c. 3.0 Ga Nsuze Group of the Pongola Supergroup of southern Africa (Fig. 1) host the oldest carbonate succession in an intracontinental setting on Earth (Mason and Von Brunn, 1977; Beukes and Lowe, 1989). The dolostones are exposed in several erosional inliers within the southern area of distribution of the Pongola Supergroup, where they are surrounded by younger Phanerozoic rocks. Siahi et al. (2016, 2017, 2018) studied in detail the sedimentological facies and geochemical composition of carbonates within the White Mfolozi inlier and suggested deposition in a tide-dominated, restricted shallow-marine environment with riverine input draining the Kaapvaal Craton.They identified a variety of microbialites on the basis of size, microfabric and morphology, suggesting potentially distinct assemblages of microorganisms responding to different physicochemical and environmental conditions. Microbialites mainly formed due to the in-situ carbonate precipitation from the water column and, to a lesser extent, the trapping and binding of clastic sediment.

Here we report on carbonate and associated siliciclastic facies from the Pongola Supergroup in the Buffalo River inlier of KwaZulu-Natal (Figs. 1 and 2; Dixon, 2004). Since the limited geochemical study of Eglington et al. (2003) of a single outcrop, no detailed facies and

* Corresponding author at: Department of Geology, University of Johannesburg, South Africa.
E-mail address: ahofmann@uj.ac.za (A. Hofmann).

https://doi.org/10.1016/j.precamres.2024.107493
Received 14 April 2024; Received in revised form 21 June 2024; Accepted 25 June 2024
Available online 14 July 2024
0301-9268/© 2024 The Author(s). Published by Elsevier B.V. This is an open access article under the CC BY license (http://creativecommons.org/licenses/by/4.0/).

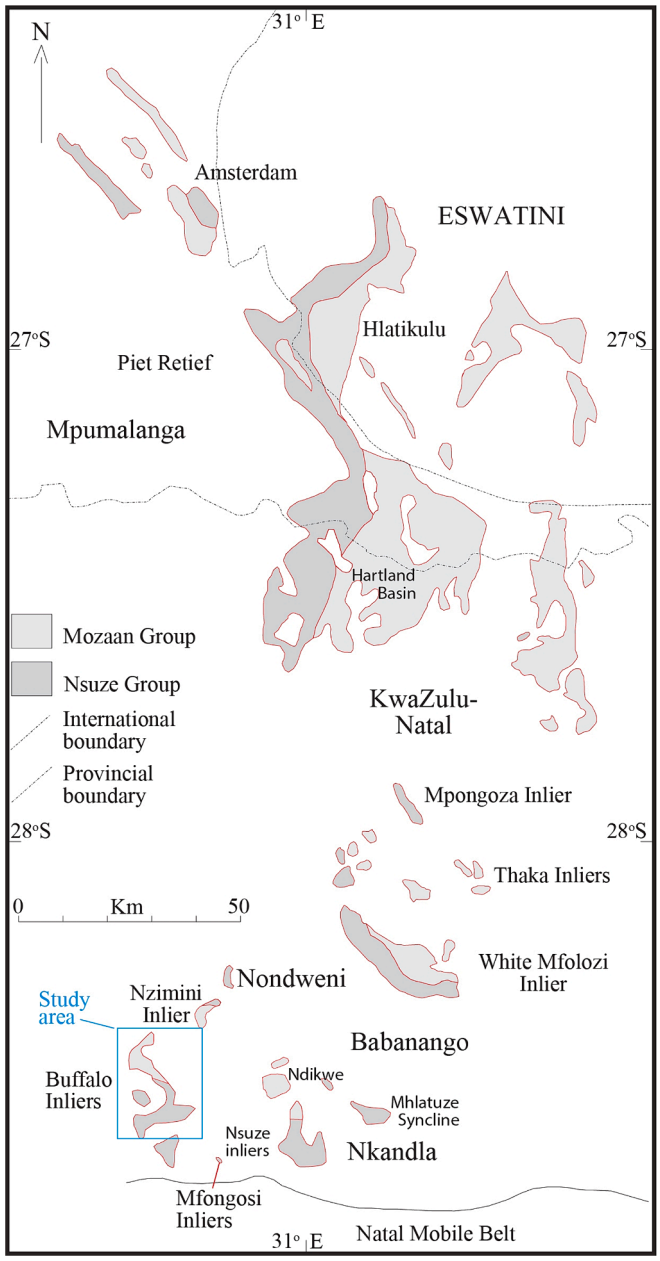

Fig. 1. Distribution of the Pongola Supergroup in South Africa and Eswatini (modified after Dixon, 2004). Rectangle shows outline of the study area (Fig. 2).

geochemical analyses have been undertaken on these rocks. This paper outlines and interprets the sedimentological characteristics and facies of several tectono-stratigraphically distinct carbonate sections in the Buffalo River inlier and their geochemical and isotopic composition with the goal to reconstruct depositional environments and to further understanding of surface processes influencing the habitat of early life.

2. Geological setting

Carbonates within the Mesoarchaean Nsuze Group, Pongola Supergroup, were first identified in the White Mfolozi inlier and were assigned to the Chobeni Formation of the Nsuze Group (Fig. 3A; Matthews, 1967; Mason and Von Brunn, 1977; Von Brunn and Mason, 1977; Siahi et al., 2016). Thereafter, carbonates within the Nsuze Group were also observed in the Nsuze (Groenewald, 1984; Hicks et al., 2011, 2021), Buffalo (Dixon, 1988, 1992, 1993, 2004) and Mhlatuze (Hicks et al., 2021) inliers. Some authors correlated the carbonate units in these various areas and reassigned them to the Chobeni Member of the White Mfolozi Formation of the Nsuze Group (Cole, 1994; Hicks et al., 2011, 2021; Wilson et al., 2013). Dixon (1992, 1993, 2004) recognized two separate carbonate-bearing successions in the Buffalo River inlier, one near the base of the Nsuze Group in the Mazebeko area (Figs. 2 and 3) associated with quartzite and minor argillite (Q1, Mdlelanga Formation) and the other in tectono-stratigraphically higher units (Nkunyana and Malakata formations) in the Mangeni area (Figs. 2 and 3), which he termed the Buffelshoek and Dent members (Dixon, 2004). He was unable to provide unequivocal evidence of their relative age.

The rock assemblages in the Buffalo River inlier have been subjected to greenschist facies metamorphism. A prominent cleavage in argillaceous dolomitic units indicates that this succession experienced open folding on a regional scale. Dixon (2004) reported evidence for at least three deformation events, (i) a compressional event involving folding and thrusting, (ii) cross-folding, and (iii) brittle faulting.

2.1. Lower carbonates

Dolostones near the base of the Nsuze Group are exposed in the Mazebeko and Mahlaba areas along tributaries of the Buffalo River (Fig. 2). In the Mazebeko area, carbonates are situated between mafic volcanic and volcaniclastic rocks (member V1) below and siliciclastic sedimentary rocks (member Q2) above (Fig. 3B). The latter consists of a succession of ~20 to 30 m thick siliciclastic sedimentary packages characterized by an increase in bed thickness, grain size and maturity up section.

Along the Mgunjane River section (Fig. 4) the volcanic rocks of unit V1 are massive to amygdaloidal and become highly schistose towards the contact with the carbonates, giving rise to a chlorite schist. Carbonates consist of strongly sheared stratiform stromatolite facies just a few metres thick (Fig. 5) that pinch out laterally due to strong deformation. The carbonates are overlain by a schistose slate with lenticular bedding that forms the base of a coarsening-upward unit capped by planar-bedded coarse quartz-arenite (Fig. 4). This is overlain by a second coarsening-upward unit. It starts with calcareous, thinly bedded, medium-grained sandstone with deformed domal stromatolites up to 3 cm in height and 20 cm in length and is capped by coarse quartz-arenite.

Along the Mazebeko River (Fig. 5) dolostones are also in sheared contact with the underlying volcanic rocks. The carbonate succession is ~13 m thick and consists largely of stratiform stromatolite facies. The carbonates here are intensely foliated and crenulated, but deformed lenticular domains suggest the former presence of small- to medium-scale domal stromatolites. The carbonate grades into a schistose silicified carbonate. Separated by a faulted contact occur schistose massive greywacke containing scattered domal stromatolites. This unit is overlain along an erosive contact by coarse-grained cross-bedded quartz arenite.

Whereas only one carbonate unit was observed within the Mazebeko area, four carbonate units have been mapped as part of stratigraphic unit Q2 in the Mahlaba area (Fig. 2; Dixon, 2004). Here, the carbonates are closely associated with siliciclastic rocks and rarely form compositionally distinct individual units. A thinly bedded to crinkly laminated sandstone with a patchy occurrence of small stromatolite domes is a common sedimentary facies. Intensely silicified former carbonate units showing traces of columnar stromatolites occur locally. No sampling was done in the Mahlaba area.

2.2. Upper carbonates

Several carbonate units are present in the northern part of the study area (Mangeni area, Fig. 2). They include the Buffelshoek and Dent sections at a yet unresolved stratigraphic level (Fig. 3). A persistent silicified carbonate up to 5 m thick and referred to as the Buffelshoek Member is characterised by stratiform stromatolite and columnar/domal stromatolite facies. It is situated at the base of the Malakatha

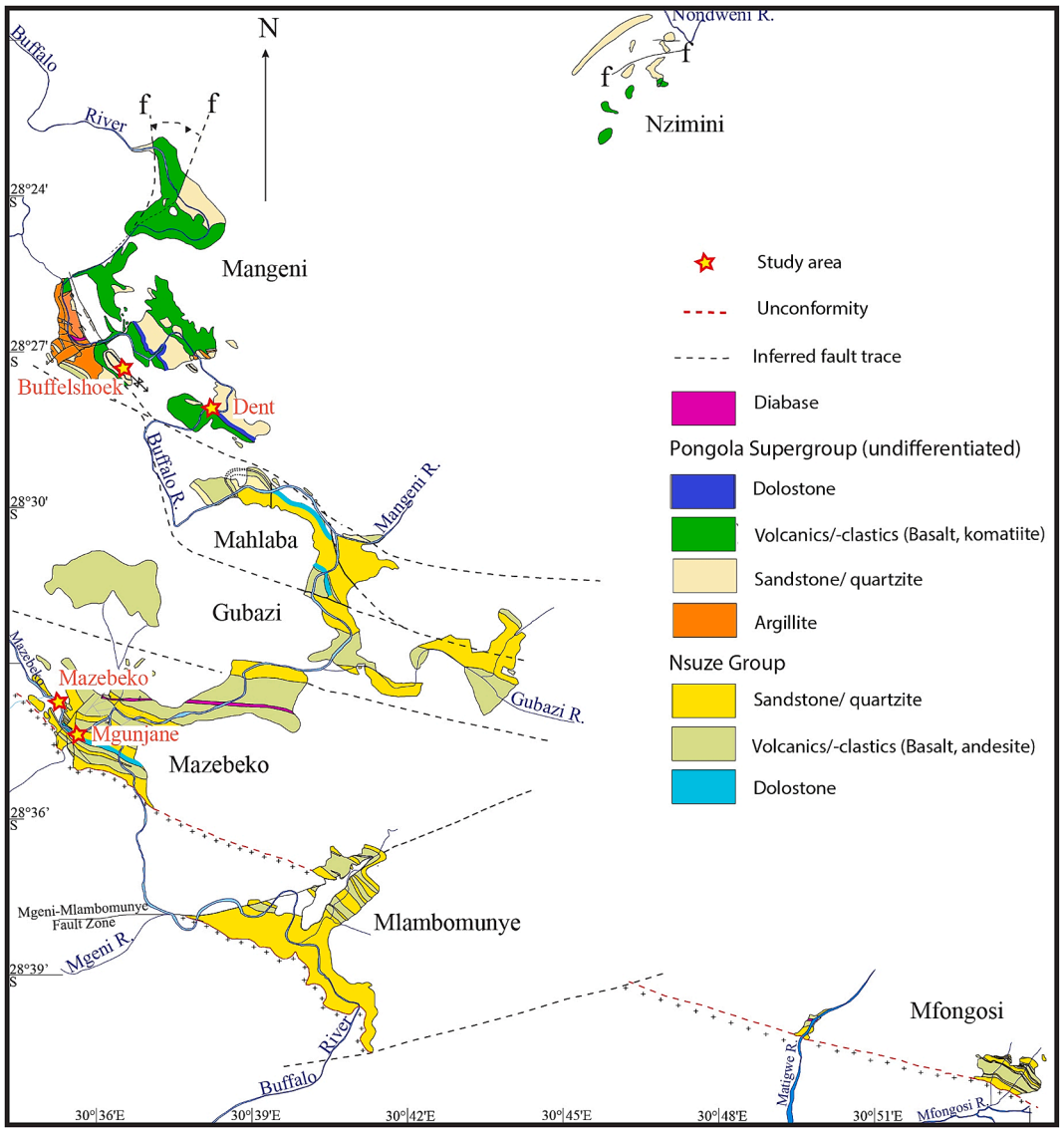

Fig. 2. Geological map of the Buffalo River inlier of the Pongola Supergroup, showing distribution of the four measured carbonate sections (modified after Dixon, 2004). Under- and overlying strata are not shown, except for basement shown as crosses.

Formation marking its contact with the underlying volcanic Nkunyana Formation (Fig. 3C). The Nkunyana Formation largely consists of volcaniclastic rocks at the base and amygdaloidal mafic volcanics at the top and is separated from underlying strata by a major fault zone (Dixon, 1992, 2004).

The Buffelshoek carbonate member is overlain by fine- to medium-grained quartz wacke/siltstone, showing planar and ripple cross-lamination, ripple marks and desiccation cracks. Argillaceous drapes veneer bedding surfaces (Fig. 3C). The overlying unit comprises medium- to coarse-grained cross-bedded feldspathic sandstones hosting two carbonate units referred to as the Dent Member (Dixon, 2004). The carbonate-sandstone association is overlain by coarse-grained quartz arenites with both planar and trough cross-bedding (Dixon, 2004). The stratigraphically highest unit (Fig. 3C) is a feldspathic sandstone. The upward continuation of this sequence is concealed by Phanerozoic cover of the Dwyka Group of the Karoo Supergroup (Dietrich and Hofmann, 2019).

Carbonates of the Dent Member were investigated at two sites, referred to the Buffelshoek and Dent sections named after the farms on which they are exposed. Characteristics of these carbonates include the presence of stratiform and minor domal stromatolites. Furthermore, the carbonates are underlain, overlain, and interbedded with largely wave-ripple laminated, fine- to medium-grained sandstones.

The Buffelshoek section exposes a single unit of carbonate (Fig. 5) along a small tributary of the Buffalo River. The carbonates are made of irregular thin to medium beds of dolostone intercalated with discontinuous lamina to thin beds of massive coarse-grained sandstone. The latter may be situated between or drape small domal stromatolites up to 5 cm in diameter.

The Dent section consists of two variably silicified units of interstratified sandstone and dolostone (Fig. 5). The first overlies amygdaloidal basalt and consists of thin to medium beds of variably silicified sandstone and carbonate with wrinkly and wavy lamination. This is overlain by a succession of wave-ripple laminated sandstone that grades into wrinkly laminated calcareous sandstone with common scattered domal stromatolites and less abundant tepee structures filled with sandstone and/or massive light grey chert.

3. Methodology

Forty representative samples were collected from four different sections of the Pongola Supergroup in the Buffalo River inlier for

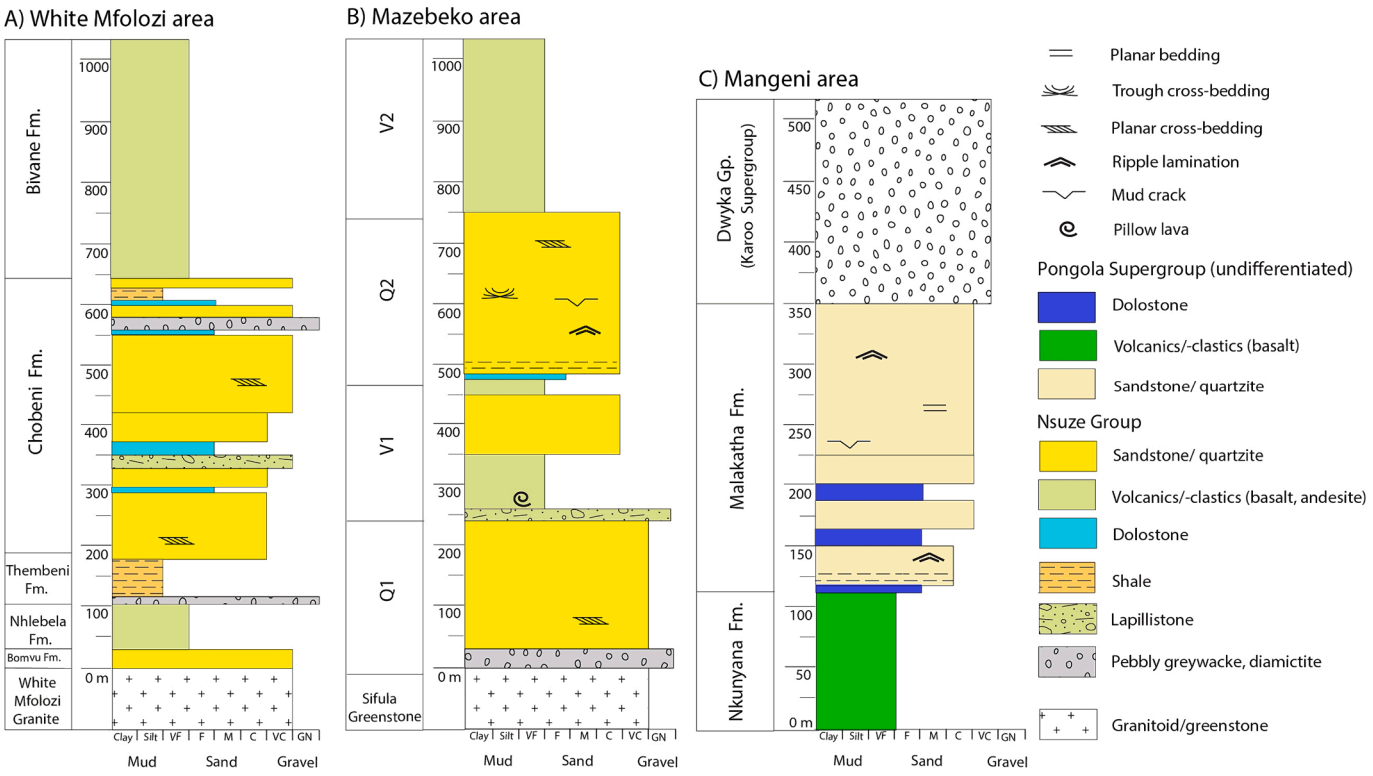

Fig. 3. Comparative stratigraphic columns of the Pongola carbonates within the type area of the White Mfolozi inlier (after Siahi et al., 2016), the basal sequence of the Nsuze Group in the Mazebeko area, and the stratigraphy of carbonate-bearing strata in the Mangeni area of the Buffalo River inlier (Dixon, 1992, 2004).

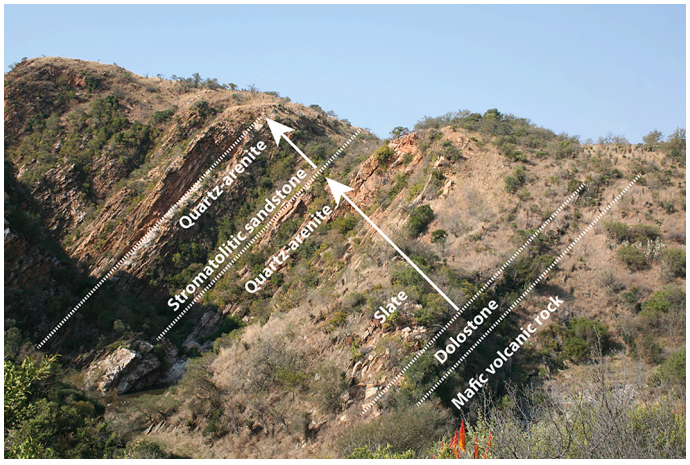

Fig. 4. Mgunjane River section. The studied succession overlies mafic volcanic rocks and is overlain by siliciclastic deposits. Arrows indicate coarsening-upward successions.

microfacies and geochemical analyses. These rocks are exposed in steep cliffs along the Buffalo River, but they did not escape weathering, as in all surface exposures. Weathering of the Pongola dolostones generally results in red to orange colouration of rock close to the surface, although visible alteration can be penetrative for several centimetres into the rock. This colour change is linked to the formation of Fe-oxyhydroxides due to the ferroan nature of the dolomite. While preference was given to samples lacking visible signs of recent weathering, not all our samples from the Buffalo River are visually pristine.

Polished thin-sections and rock slabs were studied for carbonate composition, texture, structure, and degree of preservation using binocular and petrographic microscopes. Following a detailed microfacies analyses, the best-preserved carbonate samples were selected from representative facies for bulk-rock major element chemical analysis using a PANalytical MagiX PRO wavelength-dispersive X-ray fluorescence (XRF) spectrometer at the University of Johannesburg following the protocol outlined by Siahi et al. (2018).

The trace element concentrations of carbonate samples were analysed on sample powders using two different acid leaching procedures, namely leaching by acetic acid and hydrochloric acid to evaluate possible effects of digestion of siliciclastic material on trace element concentration and distribution patterns. For non-carbonate samples, as well as for a selected suite of carbonate samples, complete acid digestion was undertaken using a mixture of HF and HNO_3 and employing the MARS (CEM) microwave digester. Analyses were undertaken at the School of Geosciences, University of the Witwatersrand, using a Perkin Elmer Sciex ELAN DRC-e inductively coupled plasma mass-spectrometer, against primary standard solutions and validated against certified

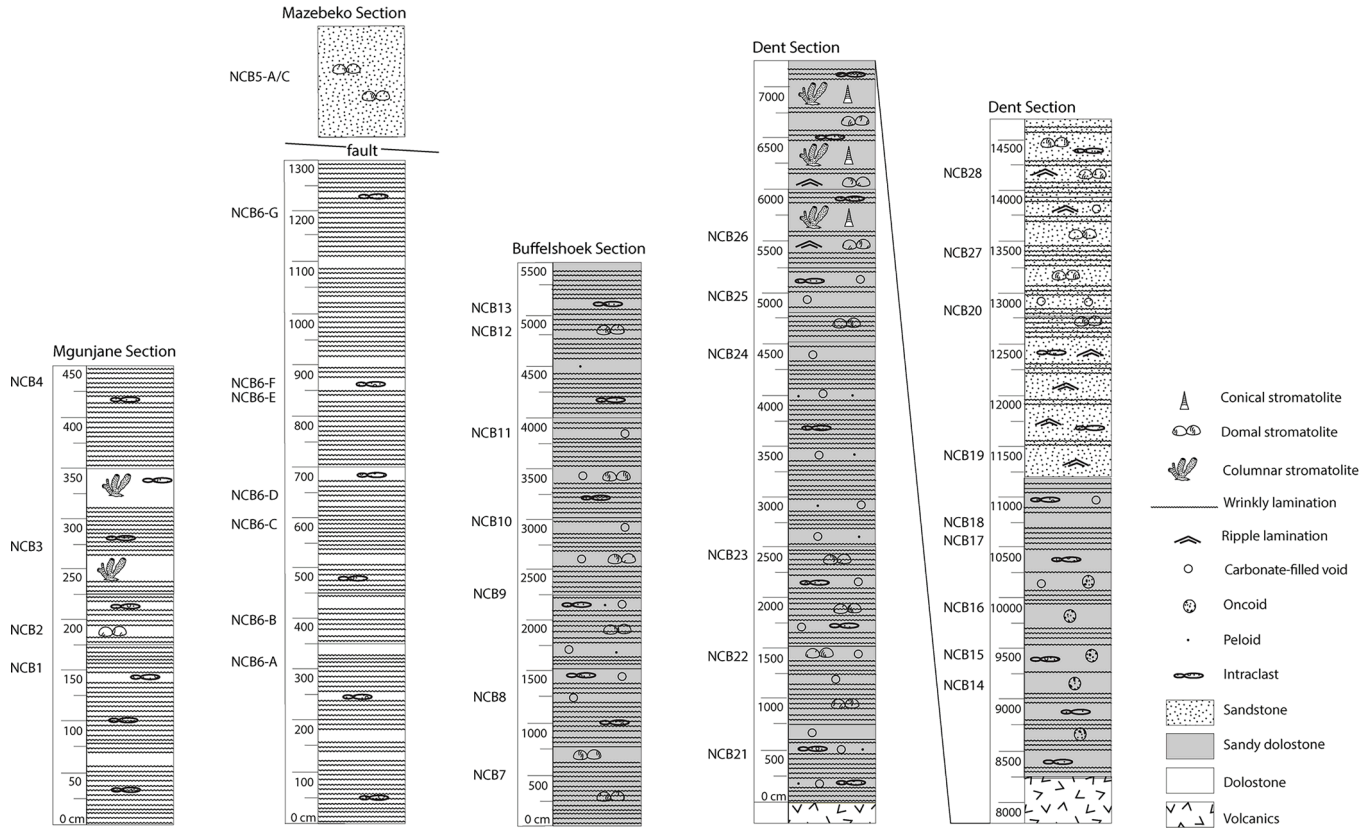

Fig. 5. Stratigraphic columns of the Mgunjane, Mazebeko, Buffelshoek and Dent sections. Sample localities are shown. Scale varies between the sections.

standard rock materials. For further details on analytical procedures refer to Siahi et al. (2018).

Eighteen whole-rock sample powders were analysed for carbon and oxygen isotopes using a Gasbench ll linked to an isotope ratio mass-spectrometer (DeltaPlus, ThermoFinnigan MAT, Bremen, Germany) at the Ludwig-Maximilian-University of Munich. Carbonate isotope ratios are reported using standard δ-notation relative to Vienna-Pee-Dee Belemnite (VPDB). International standards (NBS-18 and NBS-19) and a laboratory standard ('Pfeil') consisting of pure Solnhofen limestone were used for calibration. For further details refer to Siahi et al. (2018).

The least altered samples were selected for strontium isotope analyses. Two acid leaching procedures have been applied on the sample powders (Siahi et al., 2018). The Sr in the leachate was chromatographically separated and measured on a tungsten filament using a Spectromat-upgraded MAT 261 thermal ionization mass-spectrometer at Ludwig-Maximilian-University of Munich. The Sr isotope ratios are reported as present-day. No corrections accounting for the in-situ decay of ^{87}Rb were applied to the data.

Raman experiments were done using a WITec Alpha300R confocal Raman microscope, coupled with a frequency-doubled Nd-YAG laser at 532 nm excitation wavelength. Before each experiment, the system was calibrated using a polished silicon standard. A 20x (N.A = 0.4) Zeiss EC Epiplan objective lens was used to collect the scattered radiation and, when needed, the 50x (N.A = 0.55) Zeiss LD EC Epiplan-NEOFLUAR objective lens was used for more detailed analysis. The laser power at sample was 1 mW. A 100 μm optical fibre was used to collect the Raman scattered photons. This also acted as the entrance slit to the spectrometer. A 600 grooves/mm grating was used to disperse the Raman scattered wavelengths. Spot-by-spot analysis was done on all potential candidate material, guided by sample images. Ten acquisitions of 10 s integration time were collected per chosen spot, giving an average spectrum for each spot. Raman spectra were collected from different carbonaceous regions within the sample and different spots within each region, to quantify within-sample heterogeneity (Beyssac et al., 2002). Furthermore, measurements were done at a depth of 1 to 4 μm to at least limit interference from any transparent mineral grains in each sample and to avoid compromised sample from thin-section preparation. Post-acquisition processing was only limited to polynomial background subtraction. Spectral parameters were extracted through non-linear curve fitting using the Voight profile. Spectral fitting was done using OriginPro, version 2023b software (OriginLab, 2003).

4. Sedimentary facies characterization

The measured sections (Fig. 5) have been subdivided into five carbonate-bearing facies based on field observation (sedimentary structures and stromatolite type) and sample petrography. These include (1) stratiform stromatolite facies, (2) columnar/conical stromatolite facies, (3) domal stromatolite facies, (4) ripple-laminated arenaceous dolostone facies and (5) oncolite facies. The stratiform and small-scale domal stromatolite facies are widespread facies developed in the four sections, whereas columnar/conical stromatolite facies are present only at the Mgunjane and Dent sections and ripple-laminated dolomitic sandstone and oncolite facies occur only at the Dent section. A stromatolitic sandstone facies (6) was encountered in several places stratigraphically above the measured carbonate sections.

4.1. *Stratiform stromatolite facies*

Stratiform stromatolite is the most common facies in all four sections (Fig. 5). It consists of micritic to sparitic and silicified wrinkly laminae alternating with peloidal dolarenite laminae, the latter sometimes preserving ripple lamination (Fig. 6A-C). Small-scale domal stromatolites up to a centimetre in width and height are common; their internal structures usually are obscured due to diagenesis (Fig. 6D). Peloidal dolarenite laminae alternate with micritic laminae. They contain

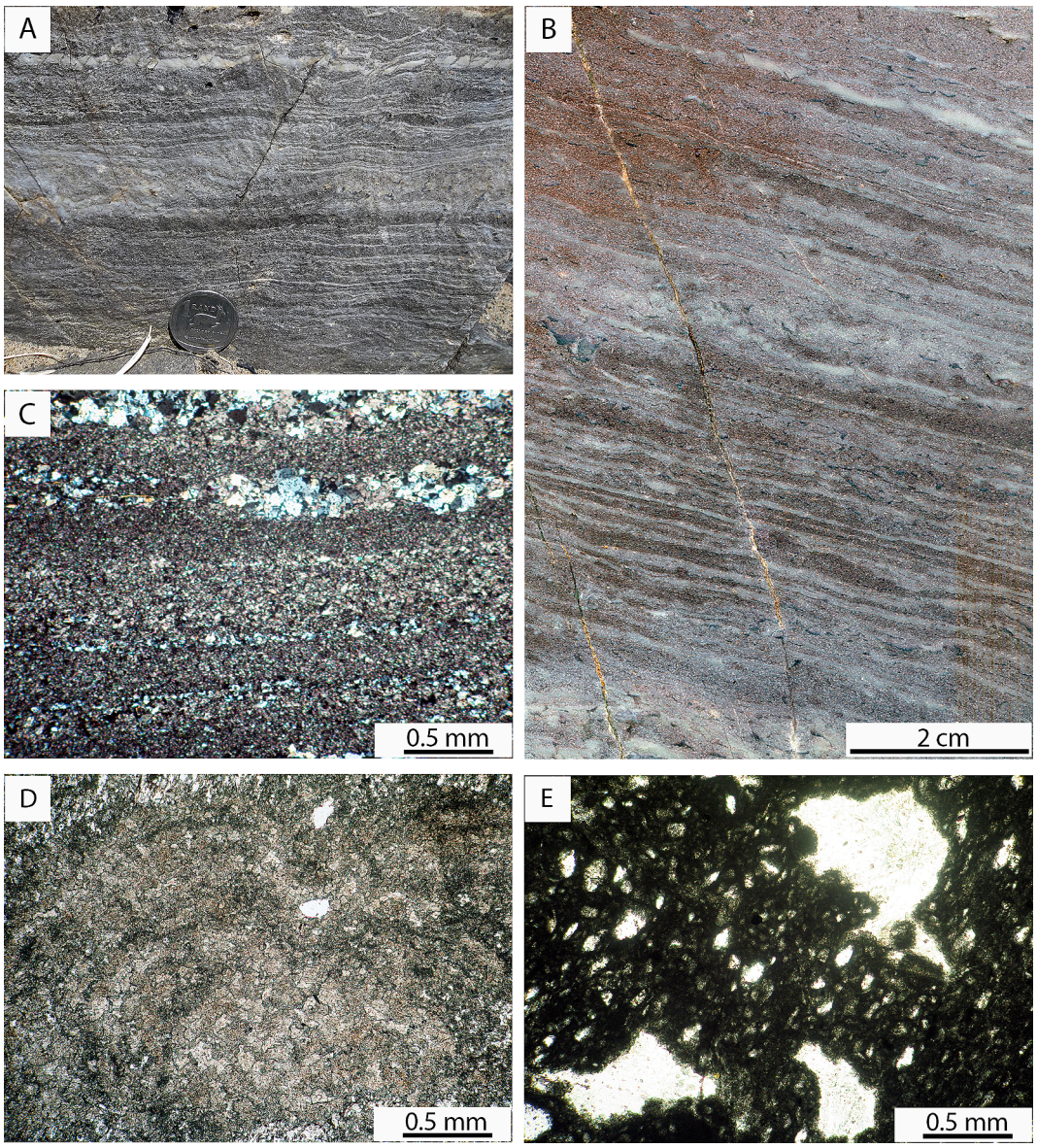

Fig. 6. Features of the stratiform stromatolite facies. (A) Field photo of the intensely silicified wrinkly laminae alternate with micritic laminae. (B) Polished slab of alternating silicified and micritic wrinkly laminae. (C) Photomicrograph (cross-polarized light) of alternating silicified, micritic and sparitic wrinkly laminae. (D) Photomicrograph (cross-polarized light) of millimeter-scale, laterally linked domal stromatolites; recrystallization resulted in the loss of internal structures. (E) Peloidal dolarenite with calcite-filled fenestrae (plane-polarized light).

partially silicified, structureless, sub-spherical micritic peloids that range from 0.05 to 0.2 mm in diameter, moderately sorted, fine to medium sand-sized quartz grains, minor euhedral pyrite, and intraclasts. Another common feature is the occurrence of spar-filled fenestrae (Fig. 6E). Rare carbonaceous matter is concentrated along silicified laminae.

4.2. Columnar/conical stromatolite facies

This rare facies is developed in the Mgunjane and Dent sections and typically alternates with stratiform stromatolite facies. It consists of partially to completely silicified sandy dolarenite/intradolorudite that hosts columnar/conical stromatolites. Columnar stromatolites are up to 15 cm in height and 5 cm in width (Fig. 7A) and consist of alternating silicified laminae with micritic laminae, which are disrupted occasionally. Conical stromatolites are up to 6 cm in height and up to 2 cm in width (Fig. 7B). Synoptic relief ranges from 2 to 5 cm.

4.3. Domal stromatolite facies

This facies in the Mazebeko and Dent sections consists of small- to medium-scale (from 1 cm up to 15 cm in diameter), isolated to laterally-linked domal stromatolites set in a groundmass of dolomitic sandstone (Fig. 7C-D). They consist of alternating silicified and micritic laminae, which are disrupted occasionally. The internal structures may range from wavy irregular lamination to a clotted fabric (Fig. 7E). The domal stromatolites often alternate with stratiform stromatolites. Domes may include, or are surrounded by, poorly sorted, fine to coarse sand-sized quartz grains.

4.4. Ripple-laminated arenaceous dolostone facies

This facies is well-developed in the Dent section and consists of thinly bedded, wave-ripple-laminated to wrinkly laminated sandy dolostone to dolomitic sandstone (Fig. 7F). It contains small- to medium-scale, patchily distributed domal stromatolites, up to 20 cm width and 15

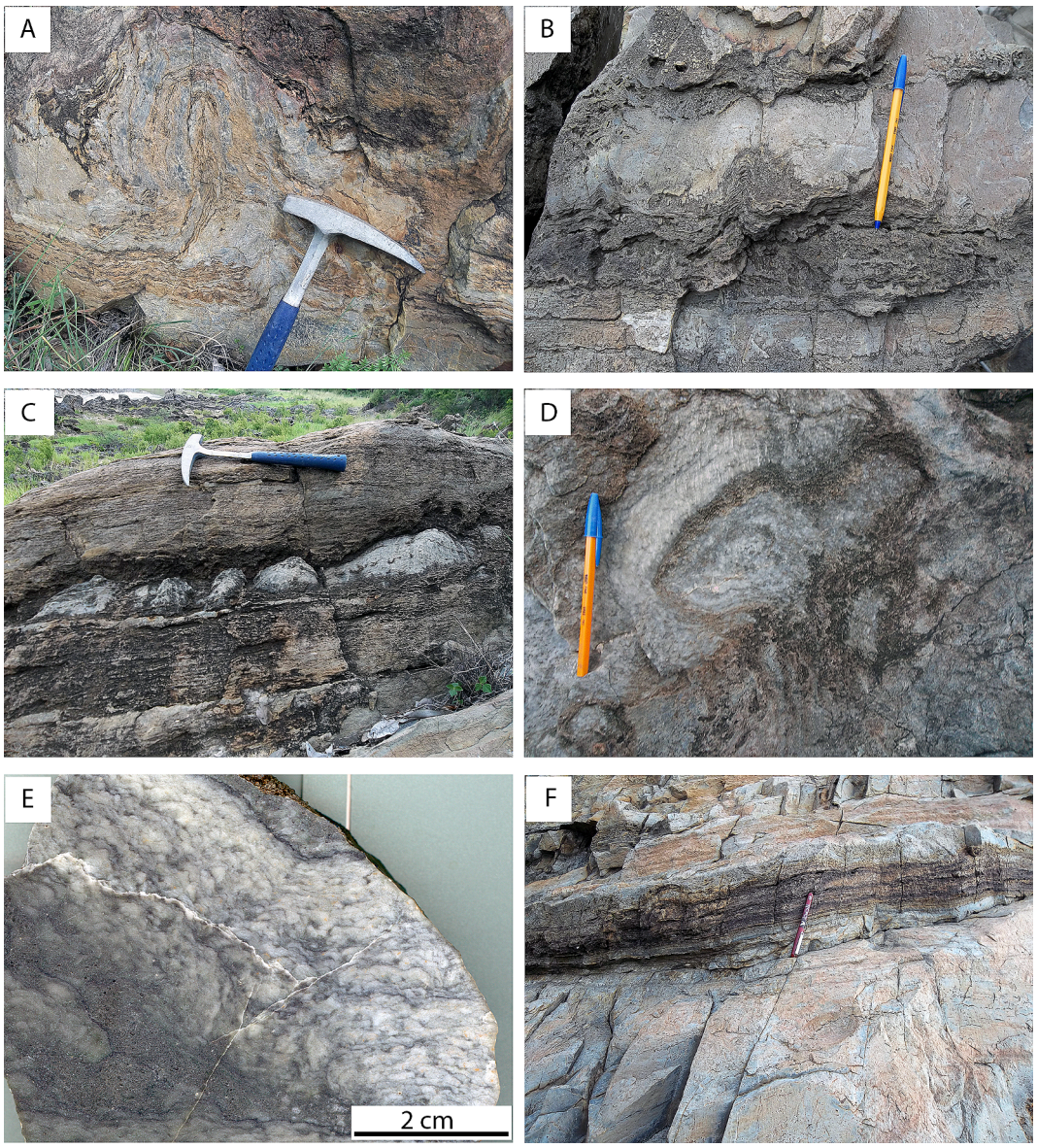

Fig. 7. Features of different lower intertidal to subtidal facies. (A) Partially silicified columnar stromatolite. (B) Silicified conical stromatolite interbedded with silicified dolarenite. (C) Laterally-linked domal stromatolites interbedded with dolomitic sandstone. (D) Plan view of partially silicified laterally-linked domal stromatolites. (E) Polished slab of a domal stromatolite with an irregularly laminated to clotted fabric. Dark domains are rich in siliciclastic detritus. (F) Ripple-laminated arenaceous dolostone facies.

cm height/synoptic relief, which are typically silicified.

4.5. Oncolite facies

This facies is only developed in the Dent section. Oncoids occur as spherical to sub-spherical grains up to 1 cm in diameter, in which dominantly micritic nuclei are coated by asymmetric to irregular concentric micritic/silicified laminae (Fig. 8). The oncoids largely lost their internal texture due to recrystallization and silicification. Other components include silicified micrite rip-up clasts (disrupted stratiform stromatolites) and quartz sand grains.

4.6. Stromatolitic sandstone facies

The stromatolitic sandstone facies was observed in the Mazebeko section and at Mtaba Mhlope in the Mahlaba area (Fig. 2). It also is a common facies in rocks above the Dent section. It typically consists of small- to medium-scale, isolated to laterally-linked domal to columnar stromatolites from 1 cm up to 15 cm in diameter set in a groundmass of massive sandstone (Fig. 9A-C). These may coalesce in places forming composite domes up to 1 m across. Synoptic relief may reach 15 cm. The matrix in the Mazebeko section is greywacke and largely made of poorly sorted medium sand-sized quartz grains, rare detrital muscovite, metamorphic chlorite, and patchily distributed dolomite. Some compacted, coarse sand-sized lapilli are present (Fig. 9D). The lapilli are largely made of chlorite, are non-vesicular and may contain quartz sand particles possibly entrained during lava/sediment interaction at the source of the ejecta. Similar material has been described from the White Mfolozi carbonates (Siahi et al., 2016).

5. Composition and metamorphic grade

The dominant mineral in all sections is dolomite. Calcite is a minor phase and present only as secondary void-filling carbonate. The dolostones are nevertheless rarely monomineralic. Beside a variety of allochems, they contain siliciclastic detritus, rare pyroclastic particles as

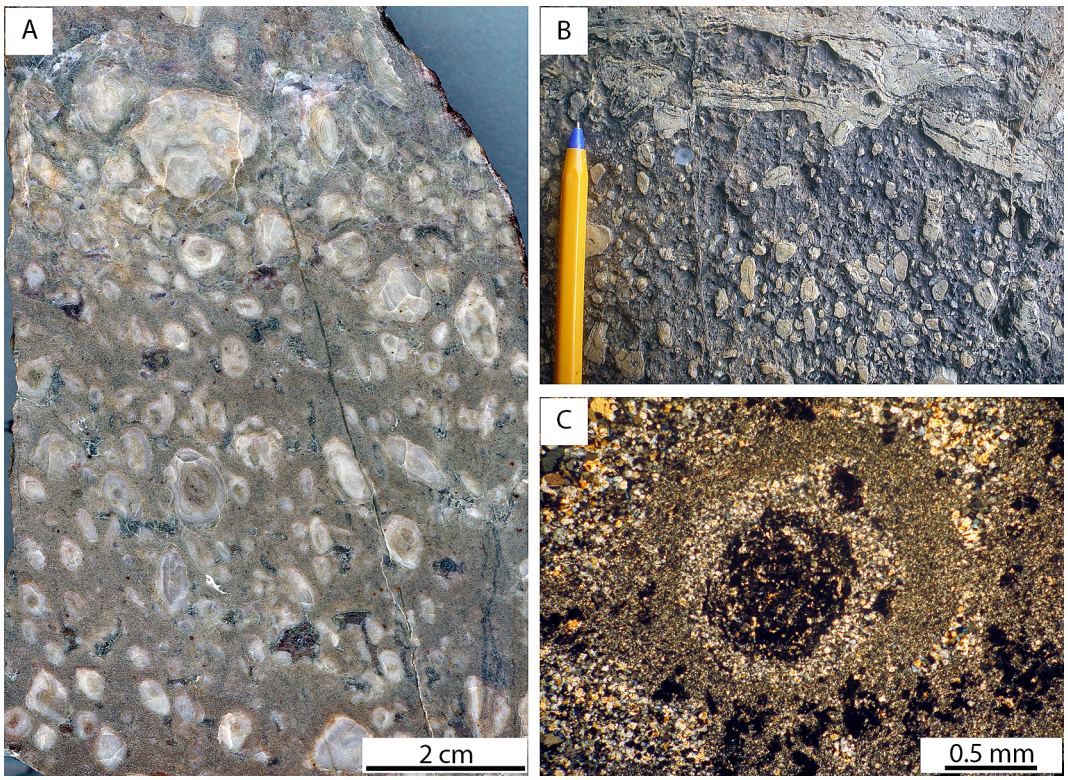

Fig. 8. Features of oncolite facies. (A) Polished slab showing mostly asymmetrical oncoids in a micritic matrix. (B) Dolorudite containing oncoids and silicified ripped-up carbonate clasts at the top of image. (C) Photomicrograph (cross-polarized light) showing partially silicified symmetrical oncoid. Dark material represents partially weathered Fe-carbonate concentrated in its nucleus.

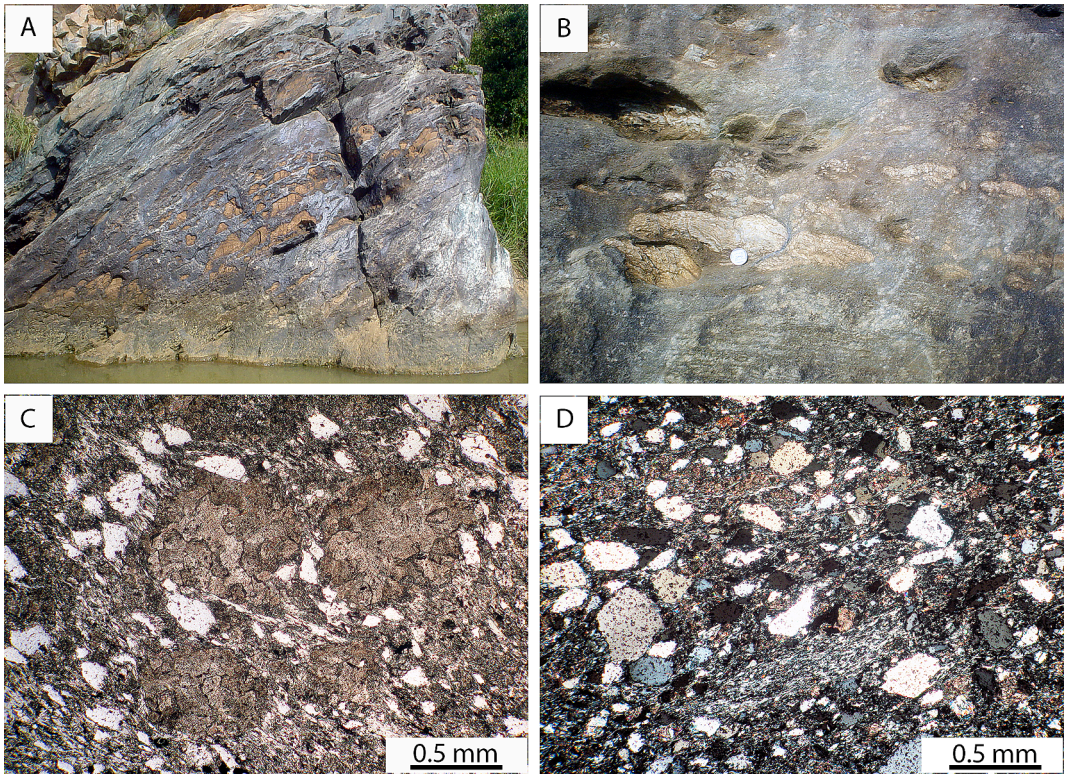

Fig. 9. Stromatolitic sandstone facies. (A) Isolated to laterally-linked domal to columnar stromatolites embedded within greywacke. Cliff is about 2 m high. (B) Close up image of outcrop shown in A. Coin for scale. (C) Photomicrograph (plane-polarized light) of isolated recrystallized very small-scale domal stromatolites embedded within greywacke. (D) Photomicrograph (cross-polarized light) of greywacke with stretched lapilli replaced by chlorite.

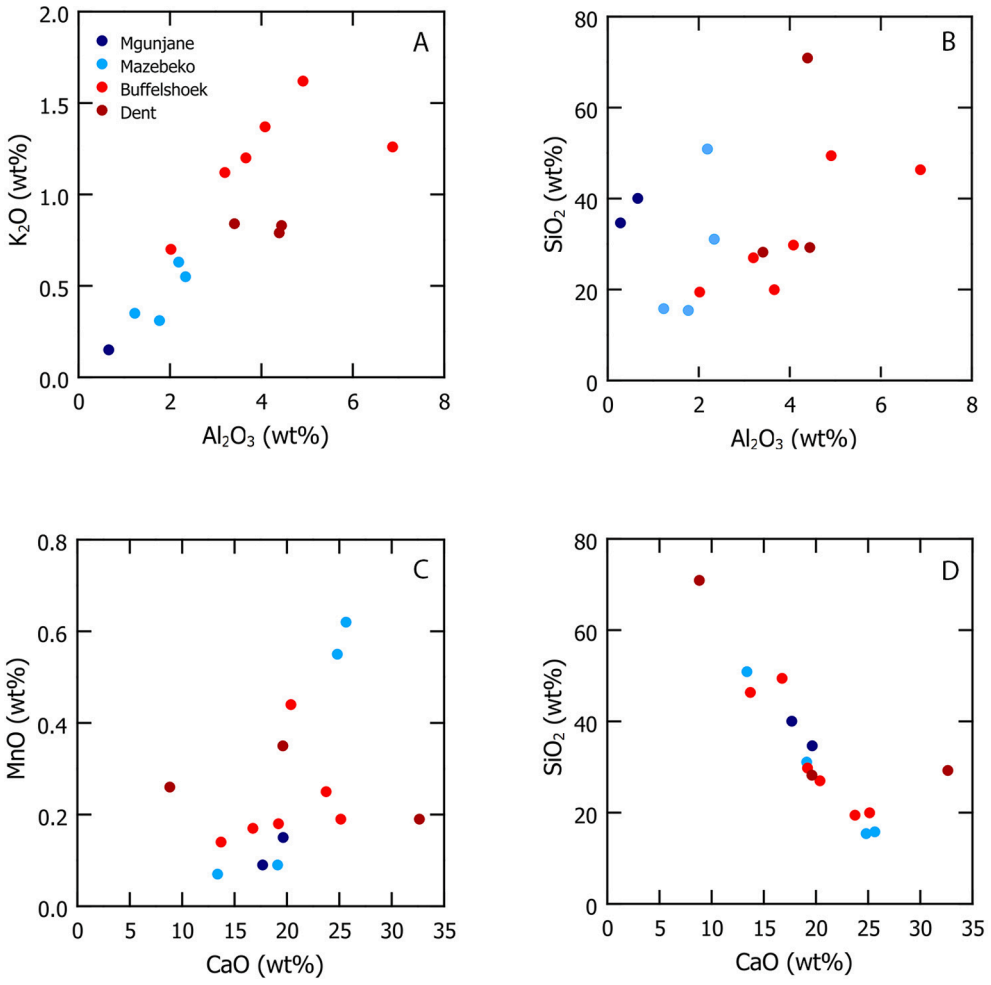

Fig. 10. (A) Al_2O_3 vs. K_2O. (B) Al_2O_3 vs. SiO_2. (C) CaO vs. MnO. (D) CaO vs. SiO_2.

well as secondary diagenetic and metamorphic phases. Allochems include peloids, ooids, oncoids, and various intraclasts very similar to those described by Siahi et al. (2016) from the White Mfolozi inlier, although rather less-well preserved. Siliciclastic detritus is composed of sub-angular to rounded, sand-sized quartz. Feldspar was not observed but may have been preferentially replaced by carbonate. Detrital muscovite flakes are common to rare. Accessory detrital heavy minerals mainly include rutile and zircon. Clastic grains are concentrated in detritus-rich laminae, but also occur as disseminated particles in carbonate. Early diagenetic features include calcite-filled voids/fenestrae. Metamorphic phases include quartz, sericite, muscovite, and chlorite. Disseminated euhedral pyrite crystals may also have formed during metamorphism. Carbonaceous matter is rare, and largely disseminated in micrite.

The carbonates have been variably affected by deformation that gave rise to small-scale folding and the development of an axial-planar foliation. In thin-section, siliciclastic and carbonate grains frequently occur as elongate crystal aggregates oriented parallel to the foliation. The foliation is defined by elongate quartz grains and a preferred orientation of phyllosilicates.

5.1. Major element composition

Major element analysis was done on bulk samples. Correlation among major elements indicates two compositionally distinct rock-forming components, a clastic phase of silicates and a carbonate phase. A positive correlation exists between the non-carbonate components, which include SiO_2, Al_2O_3, K_2O, TiO_2, and, to a large extent, Fe_2O_3, whereas their correlation with the carbonate constituents, which include CaO, MgO, MnO, and CO_2 (measured as loss of ignition, LOI, Table S1) are negative (Fig. 10). The Buffelshoek and Dent sections have much higher Al_2O_3 and K_2O concentrations compared to the Mgunjane and Mazebeko sections, indicating a much higher siliciclastic component. In the latter two sections, Fe_2O_3 is positively correlated (R^2 = ~0.5) with other carbonate-hosted element oxides, indicating the presence of ferroan dolomite.

A broadly positive correlation of SiO_2 with Al_2O_3 is indicative of SiO_2 being hosted mainly by Al-bearing silicates in varying proportions, in addition to detrital quartz giving rise to high SiO_2 concentrations (Fig. 10). The positive correlation between Al_2O_3 and K_2O suggests the presence of detrital K-feldspar (or their alteration products) and detrital/metamorphic K-bearing phyllosilicates. A similar pattern applies to TiO_2 concentrations in which positive correlations of K_2O, Al_2O_3 and TiO_2 concentrations suggest their association with siliciclastic/volcaniclastic detritus and former clay minerals.

5.2. Trace element composition

Trace elements have been analysed by whole-rock digestion and weak (acetic) acid leach, the latter targeting carbonate phases. The first procedure may allow to provide insights into provenance of the clastic material, whereas the latter may provide information on the environment of carbonate deposition. Samples leached with HCl instead of acetic acid typically have somewhat higher concentrations (Table S1) of trace elements typically hosted in the non-carbonate fraction, suggesting partial dissolution of such phases.

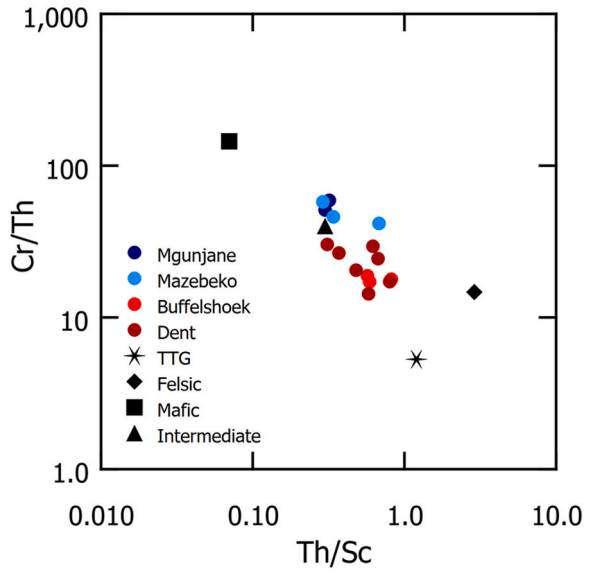

Fig. 11. Cr/Th vs. Th/Sc ratios of bulk samples in comparison with average felsic, intermediate, and mafic rock from the Nsuze Group (Nhleko, 2003) and an average composition of 3.4 Ga TTG (Hofmann, 2005).

Except for Sr, Pb and REE + Y, the much higher concentration of all other trace elements in whole-rock digestions in comparison to acetic acid leachates (Table S1) indicates that these are mostly hosted in siliciclastic detritus rather than in carbonate minerals. A comparison between LOI and the inferred carbonate-hosted elements does, however, not provide good correlations, suggesting a more complex control. Strontium concentration is variable among sections. Samples from the Mgunjane section show the highest amounts of Sr up to 379 ppm and the lowest amount is present in the Buffelshoek section with 24.5 ppm.

Absolute trace element concentrations of samples after whole-rock digestion do not provide direct insights into the origin of the rocks due to variable carbonate concentrations. Only immobile trace element ratios may provide some clues. Cr/Th and Th/Sc ratios are useful as indicators for the bulk composition of the provenance (Wronkiewicz and Condie, 1987; Hofmann, 2005). As the Nsuze Group is closely associated with volcanic rocks and overlies older granitoid-greenstone basement, we compare the composition of our samples with average felsic, intermediate, and mafic rocks from the Nsuze Group reported by Nhleko (2003) and an average composition of 3.4 Ga old tonalite-trondhjemite-granodiorite (TTG, Hofmann, 2005). Samples from the Mazebeko and Mgunjane sections have compositions similar to average intermediate Nsuze volcanic, whereas samples from the Buffelshoek and Dent sections plot between the intermediate and felsic endmembers (Fig. 11). Offsets away from the trend connecting average volcanic rock compositions can be attributed to some contribution similar in composition to average TTG.

5.3. Rare earth element composition

The concentration of rare earth elements and Y obtained from acid leachates are plotted in shale-normalized (suffix SN, Post Archaean average Australian Shale, after McLennan, 1989) diagrams (Fig. 12A). Samples prepared with different leaching procedures show approximately similar REE distribution pattern, whereas the bulk-digested sample powders have higher concentration levels, flatter patterns, and less pronounced element anomalies (Fig. 12B). The concentration levels of ΣREE in the acetic acid-leached samples vary significantly and range from c. 4.8 to 26.8 mg/kg. The average of the ΣREE in the Mgunjane, Mazebeko, Buffelshoek and Dent sections is 9.82 ± 7.16, 7.80 ± 0.48, 17.47 ± 2.64 and 26.8 ± 34.02 mg/kg, respectively. The highest ΣREE concentration (~27 mg/kg) belongs to the ripple-laminated dolomitic

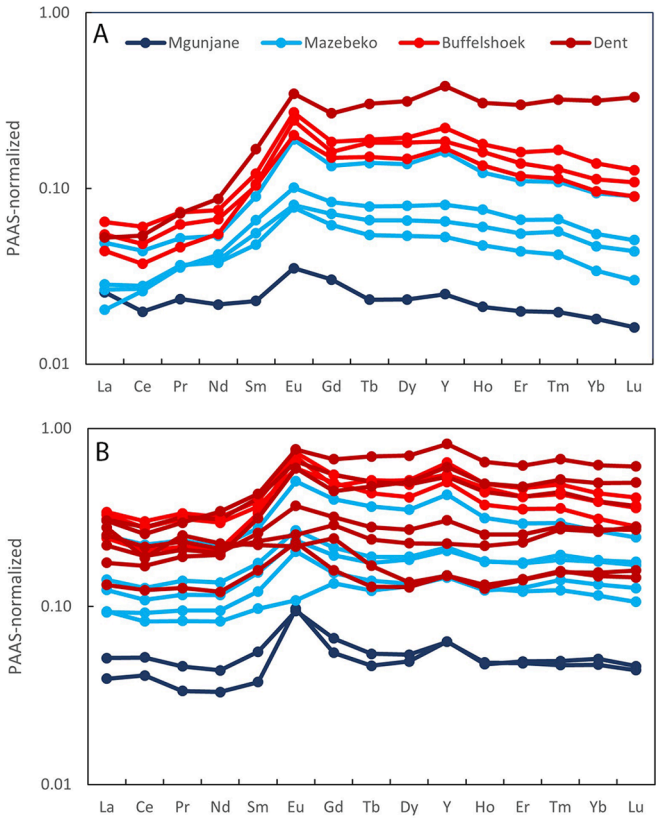

Fig. 12. PAAS-normalized REE + Y distribution pattern for (A) acetic acid-leached samples, and (B) for HF/HNO_3-digested samples.

sandstone facies. The majority of leached carbonate rock samples from the four different sections are characterized by enrichment in the middle REE (MREE; $(Pr/Tb)_{SN} < 1$ and $(Tb/Yb)_{SN} > 1$), and depleted light REE (LREE) relative to the heavy REE (HREE) calculated as [(Pr/Yb)] (Fig. 12).

Ce_{SN} anomalies are expressed as $[(Pr/Pr^*)_{SN} = Pr_{SN} / (0.5Ce_{SN} + 0.5Nd_{SN})]$ to avoid the influence of anomalous abundances of La (Bau and Dulski, 1996), and are either slightly negative with $(Pr/Pr^*)_{SN} >$

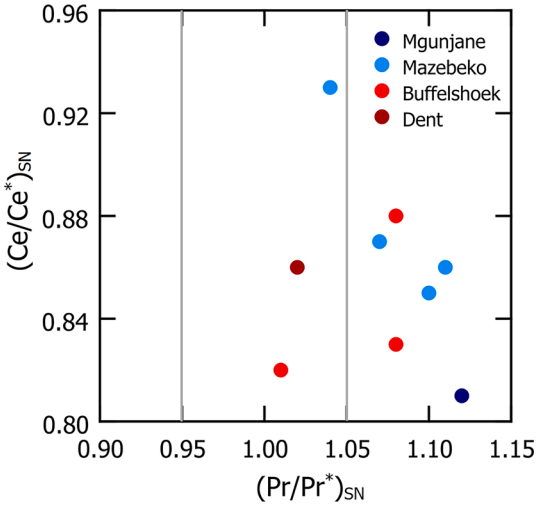

Fig. 13. $(Ce/Ce^*)_{SN}$ vs. $(Pr/Pr^*)_{SN}$ anomalies in carbonate rocks of the Buffalo River inlier (calculations according to Bau and Dulski, 1996). Centre field: positive La_{SN} anomaly, no Ce_{SN} anomaly; Right field: negative Ce_{SN} anomaly. Note that carbonate samples from four sections fall mainly into the right field.

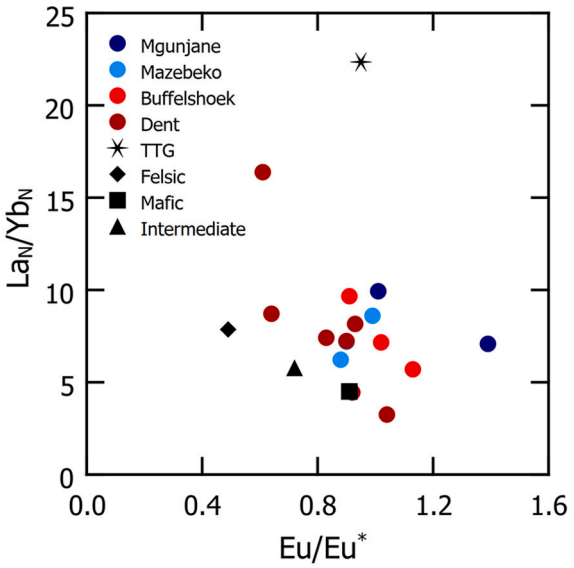

Fig. 14. Plot of Eu/Eu* vs. La_N/Yb_N of bulk samples in comparison with average felsic, intermediate, and mafic rock from the Nsuze Group (Nhleko, 2003) and an average composition of 3.4 Ga TTG (Hofmann, 2005).

1.05 up to 1.12 in several samples, or absent (Fig. 13). La_{SN} shows positive anomaly for most samples based on the combination of $(Ce/Ce^*)_{SN} < 1$ calculated as $[(Ce/Ce^*)_{SN} = Ce_{SN} / (0.5La_{SN} + 0.5Pr_{SN})]$, and $(Pr/Pr^*)_{SN} \leq 1$, as suggested by Bau and Dulski (1996). A positive Gd_{SN} anomaly calculated as $[(Gd/Gd^*)_{SN} = Gd_{SN} / (0.33Sm_{SN} + 0.67Tb_{SN})] > 1$ (after Bau and Dulski, 1996), is present in all samples. Eu_{SN} displays a positive anomaly (in all samples) calculated as $[(Eu/Eu^*)_{SN} = Eu_{SN} / (0.67Sm_{SN} + 0.33Tb_{SN})] > 1$ (after Bau and Dulski, 1996). Y is elevated relative to Ho in these carbonate rocks, as the Y/Ho ratio ranges from 29.1 in Mazebeko to 35.6 in Mgunjane, which is higher than the Y/Ho ratio for chondrite (~26–28) but much lower than the Y/Ho ratio of modern seawater (~58, Nozaki et al., 1997).

Chondrite-normalized REE concentrations of whole-rock samples show smoothly fractionated REE patterns with slight LREE enrichment (La_N/Sm_N = 2.43–5.43) coupled with slight HREE depletion (Gd_N/Yb_N = 1.20–2.13). Most samples have a small negative Eu anomaly (average Eu/Eu* = 0.94). The REE signatures are similar to those of average Nsuze Group volcanic rocks (Fig. 14), although higher La_N/Yb_N ratios indicate the presence of detritus similar in composition to average TTG. Nevertheless, REE patterns between potential source rocks and the rocks investigated here cannot be directly compared due to the influence of carbonate precipitates. The REE + Y budget is dominated by the carbonate fraction that differs in REE patterns from the clastic component (e.g., positive vs. negative Eu anomalies compared to chondrite), thus diminishing their value for provenance studies.

5.4. Carbon and oxygen isotope ratios

The carbon and oxygen isotope values of our samples overlap the range of data for carbonate samples previously reported by Eglington et al. (2003) from the study area and from the White Mfolozi inlier by Siahi et al. (2018) although they are typically somewhat lower (Fig. 15). The $\delta^{13}C_{VPDB}$ values of carbonate samples from the four sections range from −2.3 to 2.2 ‰. The $\delta^{13}C$ values from the Buffelshoek and Dent sections are more negative compared to those of the White Mfolozi and the other sections from the Buffalo River inlier. The $\delta^{18}O_{VPDB}$ values from the four sections largely overlap and range from −16.1 to −19.5 ‰ (Table S1). The highest $\delta^{13}C_{VPDB}$ and $\delta^{18}O_{VPDB}$ values are + 2.2 ‰ and − 16.1 ‰, respectively, and these values were measured in samples from the Mgunjane section.

5.5. Strontium isotope ratios

The $^{87}Sr/^{86}Sr$ ratios of carbonate bulk samples (Table S1) of the Mazebeko section range from 0.704 to 0.773 (n = 3), those of the Buffelshoek section range from 0.711 to 0.765 (n = 3), and those of the Dent section range from 0.719 to 0.737 (n = 3). There are no correlations between Sr and O or C isotope ratios. The least radiogenic $^{87}Sr/^{86}Sr$ ratio of 0.7044 was obtained from a sample of domal stromatolite facies of the Mazebeko section, which also shows the most positive $\delta^{13}C$ and $\delta^{18}O$ values of all samples. The most radiogenic $^{87}Sr/^{86}Sr$ isotope ratios in all of the carbonate sections were obtained from samples with the highest amount of clastic detritus, which also displays the most negative $\delta^{13}C$ and $\delta^{18}O$ values.

5.6. Raman geothermometric analysis

Raman spectroscopy was conducted on carbonaceous matter (CM) of two samples (NCB-11, stratiform stromatolite facies and NCB-23, domal stromatolite facies) collected from the Mangeni area (Fig. 5) to understand the degree of preservation of the carbonaceous matter and estimate the metamorphic grade. For comparison we also analysed a sample from the White Mfolozi inlier (NCMC, sandstone facies). Typical Raman spectra of CM have characteristic signatures at ~1200, ~1350, ~1500, ~1580 and ~1620 cm^{-1}; designated D4, D1, D3, G and D2 bands, respectively (Sadezky et al., 2005). In the present study, no discernible D3 and D4 bands were observed in the majority of spectra, as shown in the representative Raman spectra in Fig. 16 as well as the rest of the spectra in the supplementary material (Figure S1). Thus, peak temperatures (T) were determined by applying equation (1),

$$T = 445R2 + 641(\pm 50\ ^\circ C) \quad (1)$$

where R2 is a ratio of D1 band area (AD1) to the sum of AD1, D2 band area (AD2), and G band area (AG) (Beyssac et al., 2002). That is:

$$R2 = AD1/(AD1 + AD2 + AG) \quad (2)$$

All the spectral parameters and calculations leading to the peak temperatures are given in the supplementary material (Table S2). The average peak temperature for samples NCB11, NCB23 and NCMC is remarkable similar at 459 ± 50 °C, 452 ± 50 °C and 453 ± 50 °C, respectively.

6. Discussion

Two correlative sections of dolostone at two different (lower and upper) levels of the (tectono-)stratigraphy of the Pongola Supergroup in the Buffalo River inlier have been investigated (Fig. 2). There are some changes laterally in each pair of section that was investigated, although many of the differences are likely linked to structural overprints that these units experienced, thus restricting evaluation of true lateral facies variations. Both lower and upper carbonates are similar in terms of their over- and underlying strata, sedimentary facies and mineralogical, chemical and isotopic composition. As such, they may represent the same, but tectonically duplicated stratigraphic unit. Obvious differences in thickness and composition could thus be explained by the currently exposed sections having formed some tens of kilometres apart initially before becoming tectonically juxtaposed. Alternatively, they formed at entirely different stratigraphic levels in the Pongola Supergroup. Unambiguous solutions to the different scenarios cannot be provided in this study. At the very least, however, the lower carbonates may be correlated with those of the White Mfolozi inlier situated ~60 km to the northeast. This points to environmental conditions suitable for the deposition and preservation of marine carbonate rocks in a large part of the Pongola Basin during deposition of the lower part of the Nsuze Group.

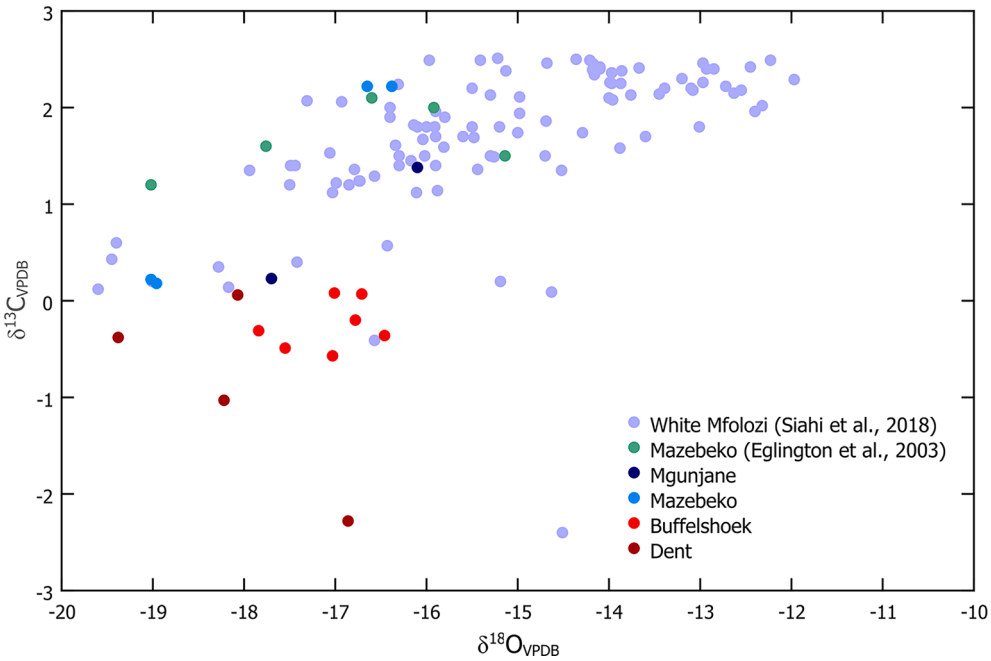

Fig. 15. Values of $\delta^{13}C$ vs. $\delta^{18}O$ for carbonate samples from the Buffalo River inlier (this study, Eglington et al., 2003) in comparison with data from the White Mfolozi inlier (Siahi et al., 2018 and references therein).

6.1. Depositional environments

The sedimentological features of the four carbonate sections support deposition in a tide-dominated shallow-marine environment. Features of the stratiform stromatolite facies, such as sediment disruption, intraclasts and fenestrae that formed due to dewatering and/or gas escape, are indicative of deposition within shallow-water with frequent subaerial exposure and desiccation (Shinn, 1986; Pratt et al., 1992; Chakrabarti et al., 2014). A supratidal/upper intertidal marine environment is indicated (Seong-Joo et al., 2000; Préat et al., 2011). The presence of ripple marks along with stratiform stromatolites refer to the more agitated, middle to lower intertidal depositional environment.

The association of columnar/conical stromatolites with coarse clastic carbonate and siliciclastic detritus suggests deposition in a submerged subtidal environment (Dravis, 1983; Grotzinger, 1989; Kah et al., 2006; Jahnert and Collins, 2012; Siahi et al., 2016). The domal stromatolites likely developed in middle-lower intertidal to shallow subtidal environments similar to their modern counterparts, which are reported from marine intertidal mudflats, protected lagoons, and shallow subtidal environments (Monty, 1967; Jahnert and Collins, 2012). The absence of sedimentary structures indicating subaerial exposure and the co-occurrence of different oncoid types (large irregular and small spherical oncoids) with clastic detritus and rip-up clasts indicate that the oncoids formed in a subtidal zone episodically influenced by storms (Logan et al., 1964; Leeder, 1975; Smith, 1986; Siahi et al., 2016). Energy levels were nevertheless relatively low due to the presence of a micrite matrix and matrix support (Fig. 8).

Arenaceous dolostone and sandstone facies intercalated with and bounding the carbonates are largely wave-swept subtidal deposits. As such, carbonates likely formed relatively near-shore, in areas protected from siliciclastic detritus as much as possible. This is very similar to carbonates in the White Mfolozi inlier (Mason and Von Brunn, 1977; Von Brunn and Mason, 1977; Beukes and Lowe, 1989; Siahi et al., 2016), where equally abundant stratiform stromatolite facies suggest a shallow-marine, tide-dominated setting.

Carbonates are thickest and best-preserved where they overlie mafic volcanic rocks. These include flows and volcaniclastics that erupted in an evolving shallow-marine to subaerial environment. Relative sea-level rise eventually resulted in the flooding of the volcanic buildup, and deposition of carbonates commenced, possibly aided initially by relatively low amounts of mobile sand-sized particles in a broadly lagoonal setting restricted from communication with the open ocean. Carbonates may thus represent transgressive deposits, in line with their preservation at the base of the shallowing-upward cycle as observed in the Mgunjane section (Fig. 4). Stromatolites present in sandstone facies higher up in the stratigraphy only form features scattered in the host rock.

6.2. Major and trace element compositions

The chemical composition of the samples reflects variable concentrations of dolomite on the one hand and siliciclastic detritus on the other. Dolomite largely controls the concentration of CaO, MgO, MnO, Sr, Pb, REE + Y and to some extent Fe_2O_3. Silicification of carbonate also played a role, but high concentrations of SiO_2 may equally reflect abundant detrital quartz. On average, carbonates from the Mgunjane and Mazebeko sections (lower carbonates) have lower concentrations of siliciclastic detritus and this may have been key for an overall better preservation of primary marine signals following diagenesis and greenschist facies metamorphism. For example, Sr concentrations are highest in the lower carbonates, the loss of which may be attributed to post-depositional alteration (Jacobsen and Kaufman, 1999; Webb et al., 2009), and similar to those observed in carbonates of the White Mfolozi inlier (Siahi et al., 2018).

6.3. Rare earth element compositions

Both leached and bulk samples show similar REE + Y patterns, although the latter have higher ΣREE concentrations and less pronounced seawater signatures which is to be expected. Much higher ΣREE in the Buffelshoek and Dent sections compared to those of in the Mgunjane and Mazebeko sections are due to their higher siliciclastic components.

The carbonate rocks from all sections show REE + Y patterns typical of Archaean seawater, including the depletion of LREE vs. HREE ($Pr/Yb < 1$), a super-chondritic Y/Ho ratio (>30), and positive Eu_{SN}, La_{SN}, Y_{SN} and Gd_{SN} anomalies (Derry and Jacobsen, 1990; Bau and Dulski, 1996;

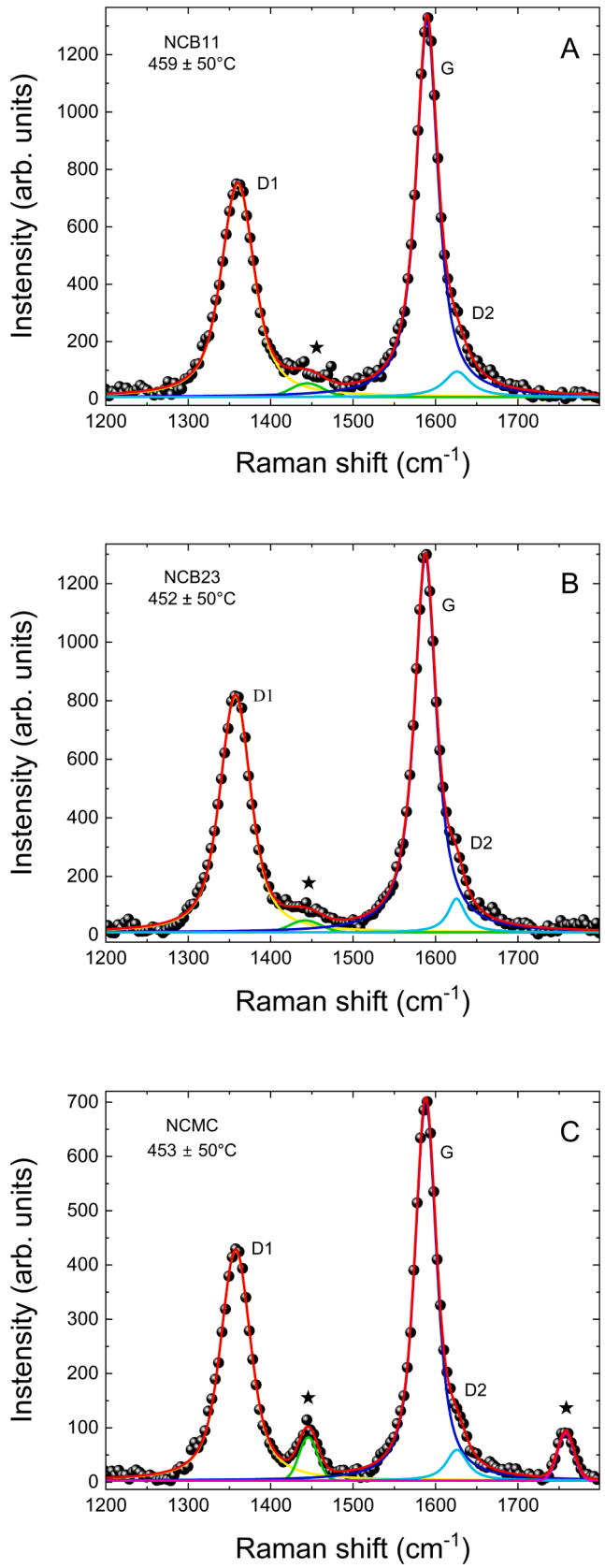

Fig. 16. Measured representative Raman spectra of carbonaceous material and corresponding average peak temperature estimates for samples (A) NCB11, (B) NCB23 and (C) NCMC. Stars show peaks from 'host' minerals in each sample.

Bau et al., 1997; Alibo and Nozaki, 1999; Kamber and Webb, 2001; Allwood et al., 2010; Hofmann et al., 2023). MREE are enriched relative to HREE and LREE in these carbonate rocks. Organic-based colloidal fractionation in rivers, coastal seas and estuaries may be responsible for MREE enrichment in such waters (Elderfield et al., 1990; Sholkovitz, 1995).

The average of $(Pr/Pr^*)_{SN}$ is slightly higher than unity in all of our samples, with some samples having a slight negative Ce_{SN} anomaly. This may be ascribed to the influence of secondary processes (Recent surface weathering) on REE patterns or deposition in slightly oxidizing environment, the latter not unlikely due to the presence of a shallow-marine oxygen oasis in the Pongola epicontinental sea (Planavsky et al., 2014; Eickmann et al., 2018).

The REE + Y patterns of the carbonates are very similar to those of the White Mfolozi inlier reported by Siahi et al. (2018). They are unlike patterns expected for an open marine setting, thus pointing to deposition in a restricted marine environment characterized by an influx of freshwater and riverine terrestrial material (Webb and Kamber, 2000; Johannesson et al., 2006; Zhao et al., 2009).

6.4. Oxygen and carbon isotopes data

The carbonate samples of the lower sections show a similar range of carbon and oxygen isotope values (Fig. 15) to those of the Mazebeko section reported by Eglington et al. (2003) and those of the White Mfolozi inlier (Siahi et al., 2018), although they are shifted towards lower $\delta^{18}O$ and $\delta^{13}C$ values suggesting a higher degree of alteration (Kaufman and Knoll, 1995; Melezhik et al., 2003; Sharp, 2007). Even lower ratios characterise the samples from the upper carbonate sections and may be attributed largely to exchange with siliciclastic components during meteoric/burial diagenesis and greenschist facies metamorphism.

6.5. Strontium isotope data

The Sr isotope ratio of seawater may be recorded in marine carbonates. However, post-depositional processes may significantly alter this ratio (Veizer et al., 1999), and this has been the case for the Pongola Supergroup carbonates. The most radiogenic Sr isotopic ratio (~0.766) was found in a sample with the highest component of clastic material from the Buffelshoek carbonate section. This is indicative of isotopic exchange of carbonate with a non-carbonate clastic component during burial diagenesis and metamorphism. The least radiogenic $^{87}Sr/^{86}Sr$ ratio of ~0.7044 was obtained from a carbonate sample from the Mazebeko section. This sample seems to have experienced relatively low degrees of secondary alteration, as it yielded the highest $\delta^{18}O$ and $\delta^{13}C$ values and contains the least amount of siliciclastic detritus. Eglington et al. (2003) reported a slightly less radiogenic $^{87}Sr/^{86}Sr$ value of ~0.7030 from the Mazebeko section. However, the primary seawater value must have been lower than that due to widespread evidence for post-depositional alteration and metamorphism of the carbonates.

6.6. Metamorphic overprint

Using Raman geothermometry, the samples from both the Buffalo River and White Mfolozi inliers share the same peak metamorphic temperature estimate of ~450 °C, which indicates greenschist facies metamorphic grade of the sampling sites. This is best attributed to regional metamorphism reported from the southeastern part of the Kaapvaal Craton at 2.72 Ga (Elworthy et al., 2000; Hofmann et al., 2015, 2019). Rocks in the Buffalo River inlier area are generally more strongly deformed, but this deformation may post-date peak metamorphism. The Buffalo River inlier is situated near the Kaapvaal Craton margin, within 25 km of the thrust front with the Mesoproterozoic Namaqua-Natal mobile belt (Fig. 1), and may have been subjected to deformation at ~1.0 Ga ago (Elworthy et al., 2000).

7. Conclusions

- Sedimentary dolostones of the Pongola Supergroup in the Buffalo River inlier of South Africa preferentially occur overlying mafic volcanic successions and are typically intercalated with shallow-marine sandstones.
- The carbonates were deposited in a tide-dominated shallow-marine environment. Different types of stromatolites formed within different sub-environments. Stratiform stromatolite formed in supra-intertidal, small-scale domal stromatolite in intertidal to subtidal and columnar and conical stromatolites in subtidal zones.
- Shale-normalized REE + Y distribution patterns of carbonate rocks are characterized by relative LREE depletion, positive La_{SN}, Gd_{SN} and Y_{SN} anomalies, and super-chondritic Y/Ho ratios, with signal magnitude indicating a restricted Archaean marine setting.
- Samples with the highest carbon and oxygen isotope values (2.2 ‰ and −16.1 ‰, respectively) contain the least amount of siliciclastic detritus. Samples with lower carbon and oxygen isotope values experienced more intense isotopic exchange with siliciclastic material during diagenesis and metamorphism. The $^{87}Sr/^{86}Sr$ ratio varies widely from 0.704 to 0.773 suggesting a moderate to strong influence of silicate detritus on the Sr isotope system during post-depositional fluid-rock interaction.
- Dolostones contain a large siliciclastic component derived from the erosion of Nsuze Group volcanics and basement TTGs.
- Environmental conditions during deposition of the lower part of the Nsuze Group were suitable for the widespread accumulation of shallow-marine carbonate rocks in the southern part of the Pongola Basin.

8. Author statement

All authors acknowledge that the material presented in this manuscript has not been previously published, nor is it simultaneously under consideration by any other journal.

CRediT authorship contribution statement

M. Siahi: Formal analysis, Writing – original draft. **A. Hofmann:** Writing – original draft, Funding acquisition, Conceptualization. **J. Dixon:** Investigation. **A. Wilson:** Methodology. **C. Mayr:** Methodology. **L. Kapesi:** Formal analysis.

Declaration of competing interest

The authors declare that they have no known competing financial interests or personal relationships that could have appeared to influence the work reported in this paper.

Data availability

All data is available in the article.

Acknowledgements

We thank Dr. Christian Reinke (University of Johannesburg), Dr. Markus Oehlerich (Ludwig-Maximilian-University, Munich) and Mr. Marlin Patchappa (University of the Witwatersrand) for assisting with XRF, IR-MS, and ICP-MS analysis, respectively. MS is grateful to Prof. Ernst Hegner for guidance during Sr isotope analysis. AH acknowledges support by the National Research Foundation of South Africa via the DSI-NRF Centre of Excellence for Integrated Mineral and Energy Resource Analysis (CIMERA) and the Centre of Excellence in Palaeosciences (Grant 86073). LK acknowledges funding by the Palaeoproterozoic Mineralization Research Group. Heinz Dedekind and staff at Elandsheim are thanked for access, advice and hospitality in the field.

Appendix A. Supplementary data

Supplementary data to this article can be found online at https://doi.org/10.1016/j.precamres.2024.107493.

References

Alibo, D.S., Nozaki, Y., 1999. Rare earth elements in seawater: particle association, shale normalization, and Ce oxidation. Geochim. Cosmochim. Acta 63 (3/4), 363–372.
Allwood, A.C., Kamber, B.S., Walter, M.R., Burch, I.W., Kanik, I., 2010. Trace elements record depositional history of an Early Archean stromatolitic carbonate platform. Chem. Geol. 270, 148–163.
Bau, M., Dulski, P., 1996. Distribution of yttrium and rare-earth elements in the Penge and Kuruman iron-formations. Transvaal Supergroup, South Africa. Precambrian Res. 79, 37–55.
Bau, M., Möller, P., Dulski, P., 1997. Yttrium and lanthanides in eastern Mediterranean seawater and their fractionation during redox-cycling. Mar. Chem. 56, 123–131.
Beukes, N.J., Lowe, D.R., 1989. Environmental control on diverse stromatolite morphologies in the 3000 Ma Pongola Supergroup, South Africa. Sedimentology 36, 383–397.
Beyssac, O., Goffé, B., Chopin, C., Rouzaud, J.N., 2002. Raman spectra of carbonaceous material in metasediments: a new geothermometer. J. Metamorph. Geol. 20, 859–871.
Chakrabarti, G., Shome, D., Kumar, S., Stephens 111, G.M., Kah, L.C., 2014. Carbonate platform development in a Paleoproterozoic extensional basin, Vempalle Formation, Cuddapah Basin. India. J. Asian Earth Sci. 91, 263–279.
Cole, E.G., 1994. Lithostratigraphy and depositional environment of the Archaean Nsuze Group, Pongola Supergroup. Rand Afrikaans University, Johannesburg, p.166. MSc thesis (unpublished).
Derry, L.A., Jacobsen, S.B., 1990. The chemical evolution of Precambrian seawater: evidence from rare earth elements in banded iron formations. Geochim. Cosmochim. Acta 54, 2965–2977.
Dietrich, P., Hofmann, A., 2019. Ice-margin fluctuation sequences and grounding zone wedges: the record of the Late Palaeozoic Ice Age in the eastern Karoo Basin (Dwyka Group, South Africa). The Depositional Record 5 (2), 247–271.
Dixon, J.G.P., 1988. Archaean geology of the Buffalo gorge. Abstr. Geocongr. Geol. Soc. S. Afr. Durban '88, 149.
Dixon, J.G.P., 2004. Archaean geology of the Buffalo River gorge. University of KwaZulu-Natal, Durban, p. 263. PhD thesis (unpublished).
Dixon, J.G.P., 1992. Unpubl. geol maps. (1:50,000 sheets 2830BC Pomeroy and 2830DA Rorkes Drift). Internal Rep. Gold Fields S.A.
Dixon, J.G.P., 1993. Lithostratigraphy of the Pongola succession in the Buffalo gorge, northern Natal. Abstr. 16th Colloq. Afr. Geol., Mbabane, Swaziland, 1, 192.
Dravis, J.J., 1983. Hardened subtidal stromatolites, Bahamas. Science 219, 385–386.
Eglington, B.M., Talma, A.S., Marais, S., Matthews, P.E., Dixon, J.G.P., 2003. Isotopic composition of Pongola Supergroup limestones from the Buffalo River gorge, South Africa: constraints on their regional depositional setting. S. Afr. J. Geol. 106, 1–10.
Eickmann, B., Hofmann, A., Wille, M., Bui, T.H., Wing, B.A., Schoenberg, R., 2018. Isotopic evidence for oxygenated Mesoarchaean shallow oceans. Nat. Geosci. 11 (2), 133–138.
Elderfield, H., Upstill-Goddard, R., Sholkovitz, E.R., 1990. The rare earth elements in rivers, estuaries, and coastal seas and their significance to the composition of ocean waters. Geochim. Cosmochim. Acta 54, 971–991.
Elworthy, T., Eglington, B.M., Armstrong, R.A., Moyes, A.B., 2000. Rb-Sr isotope constraints on the timing of late to post-Archaean tectonometamorphism affecting the southeastern Kaapvaal Craton. J. Afr. Earth Sci. 30, 641–650.
Groenewald, P.B., 1984. The lithostratigraphy and petrogenesis of the Nsuze Group northwest of Nkandla, Natal. University of Natal, Pietermaritzburg, p. 323. MSc thesis (unpublished).
Grotzinger, J.P., 1989. Facies and evolution of Precambrian carbonate depositional systems: emergence of the modern platform archetype. In: Crevello, P.D., Wilson, J. L., Sans, J.F., Read, J.F. (Eds.), Controls on Carbonate Platform and Basin Development, 44. SEPM Special Publication, Tulsa, pp. 79–106.
Hicks, N., Dunlevey, J.N., Liu, K.W., 2011. A new stromatolite occurrence in the Nsuze Group, Pongola Supergroup of Northern KwaZulu-Natal, South Africa. S. Afr. J. Geol. 114, 195–200.
Hicks, N., Gold, D.J.C., Ncume, M., Hoyer, L., 2021. A new lithostratigraphic framework and unified nomenclature for the Nsuze Group of the Nkandla sub-basin, southern Kaapvaal Craton. South Africa. S. Afr. J. Geol. 124 (3), 699–716.
Hofmann, A., 2005. The geochemistry of sedimentary rocks from the Fig Tree Group, Barberton greenstone belt: implications for tectonic, hydrothermal and surface processes during mid-Archaean times. Precambrian Res. 143, 23–49.
Hofmann, A., Kröner, A., Xie, H., Hegner, E., Belyanin, G., Kramers, J., Bolhar, R., Slabunov, A., Reinhardt, J., Horváth, P., 2015. The Nhlangano gneiss dome in south-west Swaziland - a record of crustal destabilization of the eastern Kaapvaal craton in the Neoarchaean. Precambrian Res. 258, 109–132.
Hofmann, A., Anhaeusser, C.R., Dixon, J., Kröner, A., Saha, L., Wilson, A., Xie, H., 2019. Archaean granitoid–greenstone geology of the southeastern part of the Kaapvaal Craton. In: Kröner, A., Hofmann, A. (Eds.), The Archaean Geology of the Kaapvaal Craton. Springer, Southern Africa, pp. 33–54.
Hofmann, A., Bolhar, R., Kuznetsov, A.B., Jodder, J., Butler, M., Nguyen, A., 2023. A craton-wide geochemical study of Neoarchaean carbonate rocks of Zimbabwe. Chem. Geol. 634, 121587.

Jacobsen, S.B., Kaufman, A.J., 1999. The Sr, C and O isotopic evolution of Neoproterozoic seawater. Chem. Geol. 161, 37–57.
Jahnert, R.J., Collins, L.B., 2012. Characteristics, distribution, and morphogenesis of subtidal microbial systems in Shark Bay. Australia. Mar. Geol. 303–306, 115–136.
Johannesson, K.H., Hawkins Jr., D.L., Cortés, A., 2006. Do Archean chemical sediments record ancient seawater rare earth element patterns? Geochim. Cosmochim. Acta 70, 871–890.
Kah, L.C., Bartley, J.K., Frank, T.D., Lyons, T., 2006. Reconstructing sea level change from the internal architecture of stromatolite reefs: an example from the Mesoproterozoic Sulky Formation, Dismal Lakes Group, arctic Canada. Can. J. Earth Sci. 43, 653–669.
Kamber, B.S., Webb, G.E., 2001. The geochemistry of late Archaean microbial carbonate: implications for ocean chemistry and continental erosion history. Geochim. Cosmochim. Acta 65, 2509–2525.
Kaufman, A.J., Knoll, A.H., 1995. Neoproterozoic variations in the C-isotopic composition of seawater: stratigraphic and biogeochemical implications. Precambrian Res. 73, 22–49.
Leeder, M., 1975. Lower Border Group (Tournaisian) stromatolites from the Northumberland basin. Scot. J. Geol. 11, 207–226.
Logan, B.W., Rezak, R., Ginsburg, R.N., 1964. Classification and environmental significance of algal stromatolites. J. Geol. 72, 68–83.
Mason, T.R., Von Brunn, V., 1977. 3-Gyr-old stromatolites from South Africa. Nature 266, 47–49.
Matthews, P.E., 1967. The pre-Karoo formations of the White Umfolozi inlier, northern Natal. Trans. Geol. Soc. S. Afr. 70, 39–63.
McLennan, S.B., 1989. Rare earth elements in sedimentary rocks. Influence of provenance and sedimentary processes. In: Lipin, B.R., McKay, G.A. (Eds.), Geochemistry and Mineralogy of the Rare Earth Elements. Mineral. Soc. Am, Washington, pp. 169–200.
Melezhik, V.A., Fallick, A.E., Smirnov, Y.P., Yakovlev, Y.N., 2003. Fractionation of carbon and oxygen isotopes in ^{13}C-rich Palaeoproterozoic dolostones in the transition from medium-grade to high-grade greenschist facies: a case study from the Kola Superdeep Drillhole. J. Geol. Soc. Lond. 160 (1), 71–82.
Monty, C.L.V., 1967. Distribution and structure of recent stromatolitic algal mats, eastern Andros Island. Bahamas. Ann. Soc. Geol. Belgique 90, 55–100.
Nhleko, N., 2003. The Pongola Supergroup in Swaziland. Rand Afrikaans University, Johannesburg, p. 299. PhD thesis (unpublished).
Nozaki, Y., Zhang, J., Amakawa, H., 1997. The fractionation between Y and Ho in the marine environment. Earth Planet. Sci. Lett. 148, 329–340.
OriginLab, C., 2023. OriginPro, 2023b ed. OriginLab Corporation, Northampton, MA, USA.
Planavsky, N., Asael, D., Hofmann, A., Reinhard, C.T., Lalonde, S.V., Knudsen, A., Wang, X., Ossa Ossa, F., Pecoits, E., Smith, B., Beukes, N., Bekker, A., Konhauser, O., Johnson, T.M., Lyons, T.W., Rouxel, O.J., 2014. Evidence for oxygenic photosynthesis half a billion years before the great oxidation event. Nat. Geosci. 7, 283–286.
Pratt, B.R., James, N.P., Cowan, C.A., 1992. Peritidal carbonates. In: Walker, R.G., James, N.P. (Eds.), Facies Models: Response to Sea Level Change. Geol. Assoc, Canada, pp. 303–322.
Préat, A.L., Delpomdor, F., Kolo, K., Gillan, D.C., Prian, J.P., 2011. Stromatolites and cyanobacterial mats in peritidal evaporative environments in the Neoproterozoic of Bas-Congo (Democratic Republic of Congo) and South Gabon. In: Tewari, V.C., Seckbach, J. (Eds.), Stromatolites: Interaction of Microbes with Sediments, Cellular Origin, Life in Extreme Habitats and Astrobiology, 18. Springer, pp. 43–63.
Sadezky, A., Muckenhuber, H., Grothe, H., Niessner, R., Pöschl, U., 2005. Raman microspectroscopy of soot and related carbonaceous materials: spectral analysis and structural information. Carbon 43, 1731–1742.
Seong-Joo, L., Browne, K.M., Golubic, S., 2000. On stromatolite lamination. In: Riding, R. E., Awramik, S.M. (Eds.), Microbial Sediments. Springer-Verlag, Heidelberg, pp. 16–24.
Sharp, Z., 2007. Principles of stable isotope geochemistry, 2nd Edition. Pearson Education, New Jersey, p. 344.
Shinn, E.A., 1986. Modern carbonate tidal flats: their diagnostic features. In: Hardie, L. A., Shinn, E.A. (Eds.), Carbonate depositional environments; Part 3: Tidal Flats, vol. 81. Colorado School of Mines Quarterly, pp. 7–35.
Sholkovitz, E.R., 1995. The aquatic chemistry of the rare earth elements in rivers and estuaries. Aquat. Geochem. 1, 1–34.
Siahi, M., Hofmann, A., Hegner, H., Master, S., 2016. Sedimentology and facies analysis of Mesoarchaean stromatolitic carbonate rocks of the Pongola Supergroup. South Africa. Precambrian Res. 278, 244–264.
Siahi, M., Hofmann, A., Master, S., Mueller, C.W., Gerdes, A., 2017. Carbonate ooids of the Mesoarchaean Pongola Supergroup, South Africa. Geobiology 15, 750–766.
Siahi, M., Hofmann, A., Master, S., Wilson, A., Mayr, C., 2018. Trace element and stable (C, O) and radiogenic (Sr) isotope geochemistry of stromatolitic carbonate rocks of the Mesoarchaean Pongola Supergroup: implications for seawater composition. Chem. Geol. 476, 389–406.
Smith, D.B., 1986. The Trow Point Bed-a deposit of Upper Permian marine oncoids, peloids and columnar stromatolites in the Zechstein of NE England. Geol. Soc. Lond. Spec. Publ. 22, 113–125.
Veizer, J., Ala, D., Azmy, K., Bruckschen, P., Buhl, D., Bruhn, F., Carden, G.A.F., Diener, A., Ebneth, S., Godderis, Y., Jasper, T., Korte, C., Pawellek, F., Podlaha, O.G., Strauss, H., 1999. ^{87}Sr/^{86}Sr, δ^{13}C and δ^{18}O evolution of Phanerozoic seawater. Chem. Geol. 161, 59–88.
Von Brunn, V., Mason, T.R., 1977. Siliciclastic-carbonate tidal deposits from the 3000 Ma Pongola Supergroup, South Africa. Sediment. Geol. 18, 245–255.
Webb, G.E., Kamber, B.S., 2000. Rare earth elements in Holocene reefal microbialites: a new shallow seawater proxy. Geochim. Cosmochim. Acta 64, 1557–1565.
Webb, G.E., Nothdurft, L.D., Kamber, B.S., Kloprogge, J.T., Zhao, J.X., 2009. Rare earth element geochemistry of scleractinian coral skeleton during meteoric diagenesis: a sequence through neomorphism of aragonite to calcite. Sedimentology 56, 1433–1463.
Wilson, A.H., Groenewald, B., Palmer, C., 2013. Volcanic and volcaniclastic rocks of the Mesoarchaean Pongola Supergroup in South Africa and Swaziland: distribution, physical characteristics, stratigraphy and correlations. S. Afr. J. Geol. 116, 119–168.
Wronkiewicz, D.J., Condie, K.C., 1987. Geochemistry of Archean Shales from the Witwatersrand Supergroup, South Africa: source-Area weathering and provenance. Geochim. Cosmochim. Acta 51, 2401–2416.
Zhao, Y.Y., Zheng, Y.F., Chen, F., 2009. Trace element and strontium isotope constraints on sedimentary environment of Ediacaran carbonates in southern Anhui, South China. Chem. Geol. 265, 345–362.